Study of possible ω bound states in nuclei with the (γ, p) reaction

M. Kaskulov[a], H. Nagahiro[b], S. Hirenzaki[c], E. Oset[a]

[a]Departamento de Física Teórica and IFIC, Centro Mixto Universidad de Valencia-CSIC,

Institutos de Investigación de Paterna, Aptd. 22085, 46071 Valencia, Spain

[b]Research Center for Nuclear Physics, Osaka University, Ibaraki, Osaka 567-0047 Japan

[c]Department of Physics, Nara Women's University, Nara 630-8506 Japan

February 9, 2008

Abstract

We perform calculations for ω production in nuclei by means of the (γ, p) reaction for photon energies and proton angles suited to running and future experiments in present Laboratories. For some cases of possible ω optical potentials we find clear peaks which could be observable provided a good resolution in the ω energy is available. We also study the inclusive production of $\pi^0\gamma$ in nuclei around the ω energy and find a double hump structure for the energy spectra, with a peak around a $\pi^0\gamma$ energy of $m_\omega - 100$ MeV, which could easily be misidentified by a signal of a bound ω state in nuclei, while it is due to a different scaling of the uncorrelated $\pi^0\gamma$ production and ω production with subsequent $\pi^0\gamma$ decay.

1 Introduction

The interaction of hadrons with nuclei is one of the important chapters in hadron and nuclear physics and much work has been devoted to it [1]. In particular the behavior of vector mesons in nuclei has received much attention, stimulated by the ansatz of a universal scaling of the vector meson masses in nuclei suggested in [2] and the study of QCD sum rules in nuclei [3], although earlier studies within the Nambu-Jona-Lasinio model produced no dropping of the vector meson masses [4]. More concretely, the properties of the ω meson have been thoroughly studied theoretically and different calculations have been carried out within varied models ranging from quark models, to phenomenological evaluations, or using effective Lagrangians [5, 6, 7, 8, 9, 10, 11, 12, 13, 14, 15, 16, 17, 18, 19, 20, 21, 22, 23]. The values obtained for the selfenergy of the ω in nuclei split nearly equally into attracion and repulsion and range from an attraction of the order of 100-200 MeV [9, 11] to no changes in the mass [21] to a net repulsion of the order of 50 MeV [17].

Experimental work along these lines is also rich and recently the NA60 collaboration [24] has produced dilepton spectra of excellent mass resolution in heavy ion reactions, for the spectra of the ρ, which points to a large broadening of the ρ but no shift on the mass.

On the other hand, it has been argued in [25] that reactions involving the interaction of elementary particles with nuclei can be equally good to show medium effects of particles, with the advantage of being easier to analyse. In this sense, a variety of experiments have been done with pA collisions in nuclei at KEK [26, 27, 28] and photonuclear collisions at Jefferson lab [29] by looking at dilepton spectra.

A different approach has been followed by the CBELSA/TAPS collaboration by looking at the $\gamma\pi^0$ coming from the ω decay. In this line a recent work [30] claims evidence for a decrease of the ω mass in the medium of the order of 100 MeV from the study of the modification of the mass spectra in ω photoproduction (actually, the conclusions of this paper are tied to the way the background is subtracted and it will be shown in [31] that with other justified choices of background there is no shift of the mass or it could even be positive).

With sufficient attraction, ω bound states could be produced, and could be even observable provided the ω width in the medium would not be too large. Indeed, several works have investigated the possibility to have ω bound states in nuclei [32, 9] and speculations on this possibility are also exploited in [33]. Suggestions to measure such possible states with the (d,He-3) recoilless reaction have also been made [34].

In the present work, and stimulated by the work of [33], we shall study the photon induced ω production in nuclei, looking both at the experimental set up of [33], as well as to other set ups which we consider more suited to see bound ω states with this reaction. We will make predictions for cross sections for the (γ, p) reaction in nuclei, leading to ω bound states, for several photon energies and proton angles .

At the same time we shall also present results for inclusive ω production, looking at the $\gamma\pi^0$ decay mode of the ω, as in [33], and will show that due to the presence of an unavoidable background of $\gamma\pi^0$ (unrelated to the ω) at $\gamma\pi^0$ energies smaller than the ω mass, and to the different A-mass dependence of the background and ω production, a peak develops around $m_\omega - 100 \ MeV$ in nuclei, which we warn not to misidentify with a signal of a bound ω state in the nucleus. We shall also show the optimal condictions to observe signals of eventual ω bound states, as well as the minimal experimental resolution necessary to see the possible peaks.

2   Production of bound ω states in the (γ,p) reaction

Here we evaluate the formation rate of ω bound states in the nucleus by means of the (γ,p) reaction. We use the Green function method [35] to calculate the cross sections for ω-mesic states formation as described in Refs. [36, 37] in detail. The theoretical model used here is exactly same as that used in these references.

We show first the momentum transfer of the (γ,p) reaction in Fig. 1, as a function of the incident photon energy, at forward and finite angles of the emitted proton. The momentum

transfer is the important kinematical variable which determines the experimental feasibility of the formation of meson-nuclear bound states. Indeed, deeply bound pionic atoms were discovered experimentally at the recoilless kinematics [38, 39, 34, 40]. In the formation of ω states we find that the recoilless condition is satisfied at $E_\gamma \sim 2.7$ GeV, as in Ref. [32], for ω production at threshold and forward proton production. However, the recoilless condition is never satisfied for finite proton angles. Since some experimental set ups can have problems in proton forward detection, it is interesting to determine the optimal conditions with these boundary conditions. For this purpose we look at the optimal photon energy for protons emitted with a finite angle. For an angle of $\theta_p^{\text{lab}} = 10.5$ degrees for the emitted proton, the angle measured in [33], the momentum transfer takes the minimum value at $E_\gamma \sim 1.2$ GeV. In this section, we consider 1.2 and 2.0 GeV as the incident photon energies and 0 and 10.5 degrees as the emitted proton angles in the laboratory frame.
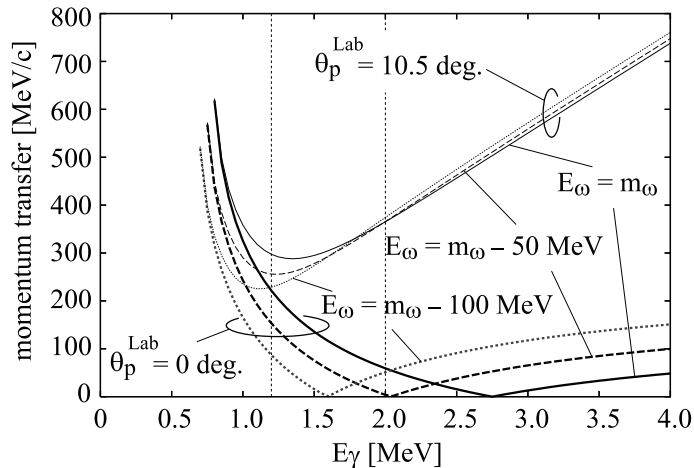

Figure 1: Momentum transfers are shown as a function of the incident photon energy E_γ in the (γ,p) reaction. The solid, dashed and dotted lines show the momentum transfers at ω energy $E_\omega = m_\omega$, $E_\omega = m_\omega - 50$ MeV and $E_\omega = m_\omega - 100$ MeV, respectively. The thick lines indicate the forward reaction cases and the thin lines the cases for the ejected proton in the final state with the finite angle $\theta_p^{\text{Lab}} = 10.5$ degree. The vertical dashed lines show the incident energies $E_\gamma = 1.2$ GeV and 2.0 GeV.

In order to calculate the cross sections at finite angles of the emitted proton, we estimate the elementary cross sections from the experimental data shown in Tables 3–5 in Ref. [41], and we use 5.0 μb/sr ($\theta_p^{\text{Lab}} = 0$ deg.) and 8.0 μb/sr (10.5 deg.) at $E_\gamma = 1.2$ GeV, and 0.7 μb/sr for both $\theta_p^{\text{Lab}} = 0$ and 10.5 deg. at $E_\gamma = 2.0$ GeV in the laboratory frame, respectively.

The ω-nucleus optical potential is written here as;

$$V(r) = (V_0 + iW_0)\frac{\rho(r)}{\rho_0}, \tag{1}$$

where $\rho(r)$ is the nuclear experimental density for which we take the two parameter Fermi

distribution. We consider three cases of the potential strength as;

$$(V_0, W_0) = -(0, 50) \tag{2a}$$
$$= -(100, 50) \tag{2b}$$
$$= -(156, 29) \tag{2c}$$

in unit of MeV. The reason for these choices is as follows. From [33] on the ω production rates in different nuclei one deduces a width for the ω at the average ω momentum in the production ($\sim 900 MeV$) and $\rho = \rho_0$ of about 100 MeV [42]. This means that the imaginary part of the potential has a strength of about 50 MeV. As discussed above, uncertainties in the subtraction of background in the experiment of [30] do not allow us to draw any conclusion on the shift of the mass [31]. Thus we have kept the possibility of a downward shift of the mass open and have performed calculations for 100 MeV binding too. We also consider the potential estimated theoretically shown in Eq. (2c), which is obtained by the linear density approximation with the scattering length $a = 1.6 + 0.3i$ fm [11]. This potential in Eq. (2c) is strongly attractive with weak absorption and hence should be the ideal case for the formation of ω mesic nuclei.

No ω bound states are expected for the potential in Eq. (2a) which has only an absorptive part. The potential in Eq. (2b) has a strong attraction with the large absorptive part as indicated in Ref. [33]. It is also interesting to compare the formation spectra obtained with the potentials in Eq. (2b) and (2c) to know the effects of the ω absorption in nuclei

We should mention here that the all spectra in this section are plotted as functions of $E_\omega - m_\omega$, while in previous papers [36, 37, 38, 39, 34] they were plotted as functions of excitation energies of final mesic-nuclear state, or equivalently, the energies of emitted particles which included the excitation energies of the core nucleus, too. We plot the spectra in this manner since we assume here experiments in which the ω meson energy can be deduced separately from the nuclear core excitation. This is the case here where the ω energy is measured by the π^0 and γ observation from subsequent ω decay $\omega \to \pi^0\gamma$ in the nucleus. We also take into account the realistic experimental energy resolution in the results.

First, we show the calculated results at $E_\gamma = 2.0$ GeV with the potential (2c) in Fig. 2. As described above, this potential is one of the ideal cases to obtain sharp signals for the mesic states formation. As we can see in Fig. 2(a), the peaks due to the mesic-nucleus formation can be seen clearly in the spectra at $\theta_p^{\mathrm{Lab}} = 0$ deg., where the momentum transfer is small as shown in Fig. 1 and the spectra are similar to those obtained in Ref. [32] as expected. Only a limited numbers of subcomponents corresponding to the substitutional states are important in this case as a consequence of the recoilless kinematics. In the spectra, we can clearly identify the ω mesic 2p state around $E_\omega - m_\omega = -50$ MeV.

On the other hand, we found the spectra with significantly different shapes at $\theta_p^{\mathrm{Lab}} = 10.5$ deg. as shown in Fig. 2(b). Because of the large momentum transfer around 350 MeV/c at this proton angle, many subcomponents have finite contributions to form the total spectrum, as shown in Fig. 2(b), and the ω production spectrum is more similar to a continuum, although only the excitation of discrete nuclear states is considered in our
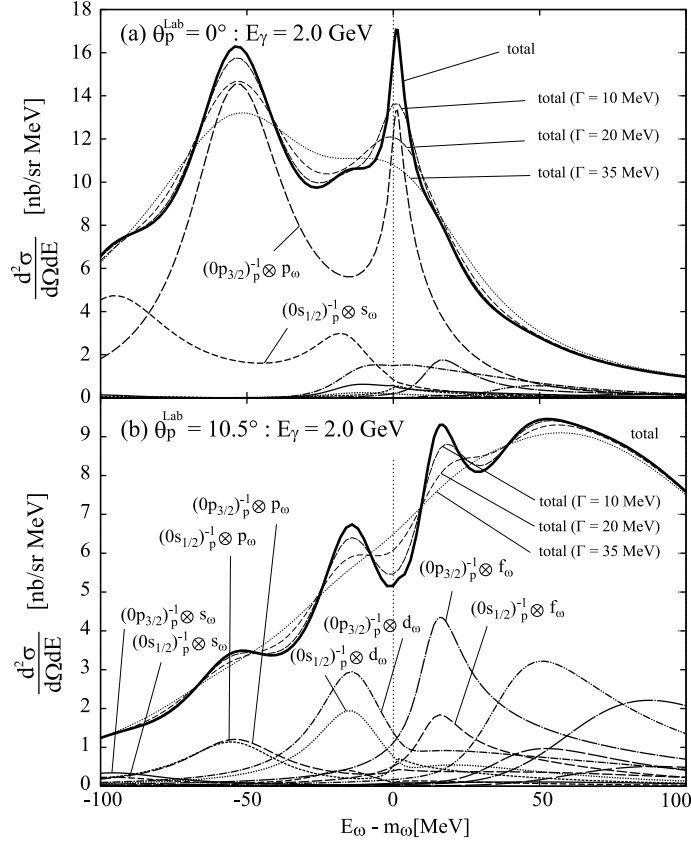
Figure 2: Formation spectra of the ω mesic nucleus in ${}^{12}C(\gamma,p)$ reaction at emitted proton angle (a) $\theta_p^{\text{Lab}} = 0$ degree and (b) $\theta_p^{\text{Lab}} = 10.5$ degree calculated with the potential depth $(V_0, W_0) = -(156, 29)$ MeV as in Eq. (2c). The incident photon energy is $E_\gamma = 2.0$ GeV. The thick solid lines show the total spectra and the dashed lines the subcomponents as indicated in the figures. The assumed experimental resolutions are also indicated in the figures.

calculations. The signals of the mesic bound states are now smaller than those at 0 degrees. Thus, it is clear that the experiments at $\theta_p^{\text{Lab}} = 0$ degrees is better suited than those at finite angles to look for the signals of ω mesic bound states at $E_\gamma = 2.0$ GeV.

In Fig. 2, we also show the expected spectra with finite experimental energy resolutions. The energy resolution is estimated to be around 35-50 MeV in a realistic case [33]. We find in the figures that the peak structures in the spectrum with the potential (2c) almost disappeared for larger experimental resolutions than $\Gamma = 10$ MeV. Thus, we conclude that an energy resolution better than 20 MeV is essentially required to obtain experimental evidence of the existence (or non-existence) of the ω mesic nucleus.

In Figs. 3 and 4, we show the calculated spectra with potentials (2a) and (2b) at $E_\gamma = 2.0$ GeV. For the potential (2a) case, we can see the enhancement of the cross section at $\theta_p^{\text{Lab}} = 0$ deg. around $E_\omega - m_\omega = 0$ MeV in Fig. 3(a). In this case, bound states do not exist and the enhancement is due to the excitation of the ω to the continuum with recoilless kinematics. At $\theta_p^{\text{Lab}} = 10.5$ deg., the enhancement is removed by the kinematical
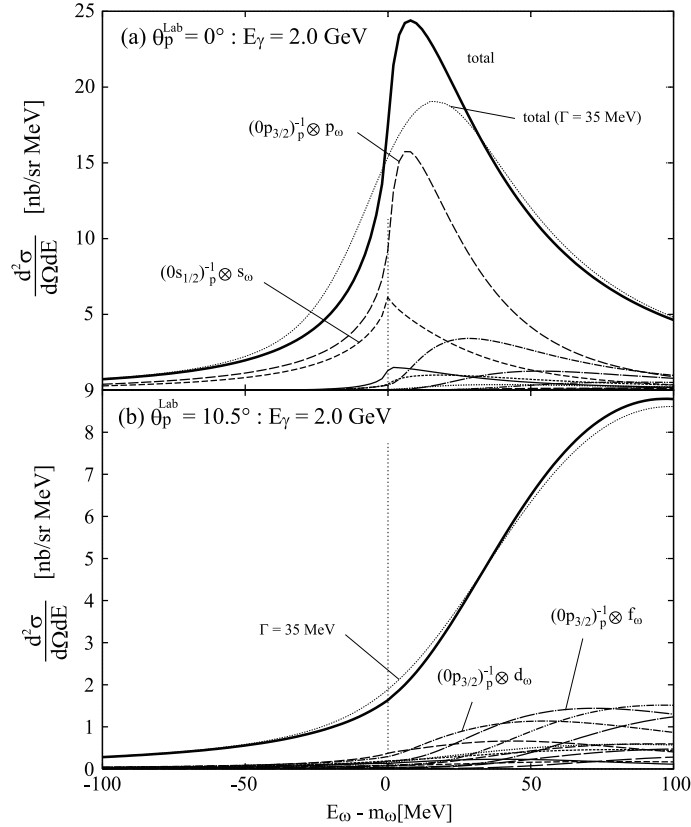
Figure 3: Same as Fig. 2 except for the potential depth $(V_0, W_0) = -(0, 50)$ MeV as in Eq. (2a).

conditions with the larger momentum transfer as shown in Fig. 3(b). In Fig. 4, the spectra with potentital (2b) are shown for $\theta_p^{\text{Lab}} = 0$ and 10.5 degrees. In this case the real part of the optical potential has enough attraction to form the bound states in the nucleus, however the imaginary part of the optical potential is also strong enough to provide a large decay width for these bound states. Thus, we can see in the Fig. 4(a) that there exists certain strength under the threshold energy which includes the contributions of the bound states formation, however, we cannot identify the binding energies neither the widths from the spectra due to the large width of the bound states. At $\theta_p^{\text{Lab}} = 10.5$ deg., we can only see a smooth slope in the spectra.

We next consider the cases with lower incident energy at $E_\gamma = 1.2$ GeV, where the momentum transfer at $\theta_p^{\text{Lab}} = 10.5$ deg. takes the smallest value as shown in Fig. 1 Theoretical investigations of this kinematics should be important to design experiments which have difficulties for the forward observation [33]. In Fig. 5 we show the results with the potential (2c) at this photon energy. As shown in Fig. 1, since the momentum transfer at 0 degree is smaller than at 10.5 degree, the signals can be seen clearer at 0 degree in Fig. 5(a) than at 10.5 degree in Fig. 5(b), as expected. However, we think it is more important to compare the spectrum in Fig. 5(b) at 1.2 GeV with that in Fig. 2(b)
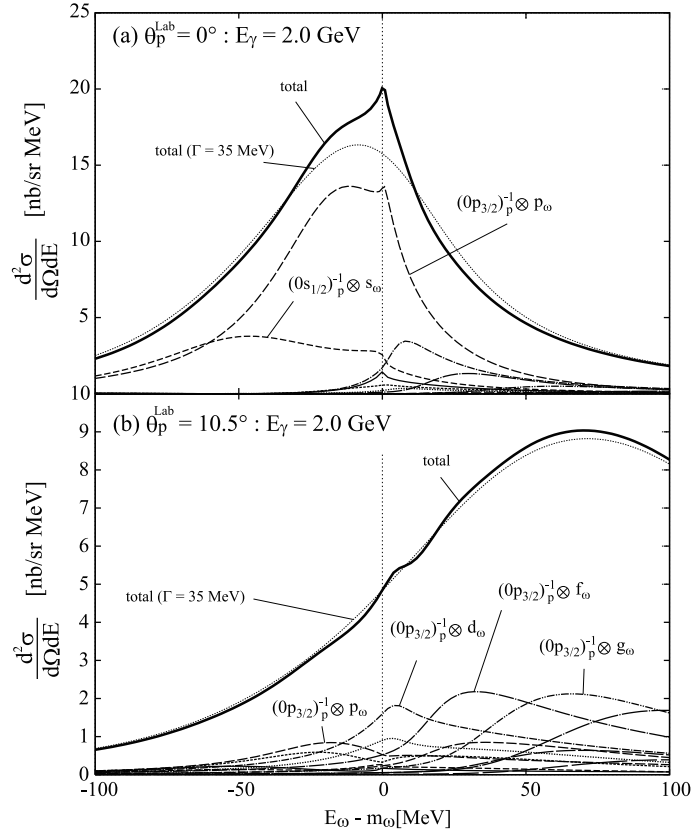
6

Figure 4: Same as Fig. 2 except for the potential depth $(V_0, W_0) = -(100, 50)$ MeV as in Eq. (2b).

at 2.0 GeV to know the better suited incident energy for the observation at finite angles of the emitted proton. We should stress that even if 2.0 GeV allows a smaller momentum transfer than 1.2 GeV when the proton is measured forward, the signals are clearer in the spectrum at 1.2 GeV than at 2.0 GeV at $\theta_p^{\text{Lab}} = 10.5$ degrees, since the momentum transfer is smaller for the lower incident photon energy. In any case, a better experimental energy resolution than about 20 MeV is required to obtain decisive information from data on the ω mesic-nucleus as mentioned above.

In Figs. 6 and 7, we also show the calculated spectra with potentials (2a) and (2b) at $E_\gamma = 1.2$ GeV. As can be seen in these figures, the spectra show a smooth ω energy dependence at this photon energy and the spectra at 0 degree and 10.5 degree resemble each other.

As a summary of this section, we would like to add few comments. In order to obtain the new information on the ω mesic nucleus we need to have the data measured with sufficiently good energy resolution, otherwise we can not conclude the existence and/or non-existence of the signals due to the mesic-nucleus formation. Furthermore, when planing to perform experiments, it is useful to consider the kinematical conditions carefully. In the cases studied here, the incident photon energy $E_\gamma = 2.0$ GeV is better suited for experiments
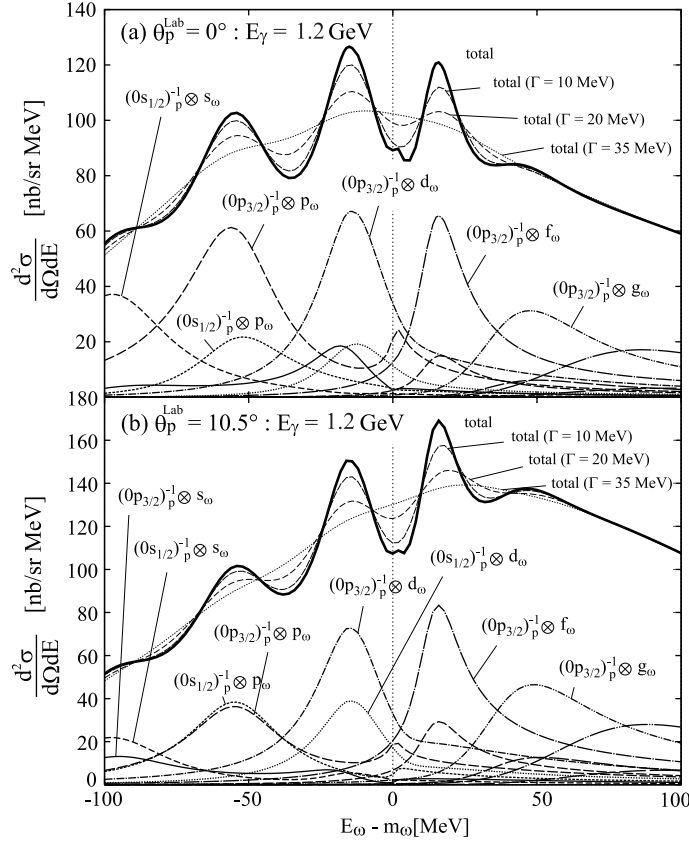
7

Figure 5: Formation spectra of the ω mesic nucleus in $^{12}C(\gamma,p)$ reaction at emitted proton angle (a) $\theta_p^{\mathrm{Lab}} = 0$ degrees and (b) $\theta_p^{\mathrm{Lab}} = 10.5$ degrees calculated with the potential depth $(V_0, W_0) = -(156, 29)$ MeV as in Eq. (2c). The incident photon energy is $E_\gamma = 1.2$ GeV. The thick solid lines show the total spectra and the dashed lines the subcomponents as indicated in the figures. The assumed experimental resolutions are also indicated in the figures.

detecting proton emission at $\theta_p^{\mathrm{Lab}} = 0$ deg, while the lower photon energy $E_\gamma = 1.2$ GeV is better suited for finite angle proton emission at $\theta_p^{\mathrm{Lab}} = 10.5$ degree.

3 Monte Carlo simulation of the reaction $\gamma A \rightarrow \pi^0 \gamma X$

In this section we perform the Monte Carlo (MC) computer simulation of the inclusive $A(\gamma, \omega \rightarrow \pi^0\gamma)X$ reaction from different nuclei. The method used here (see for the details Ref. [31]) combines a phenomenological calculation of the intrinsic probabilities for different nuclear reactions, like the quasielastic and absorption channels, as a function of the nuclear matter density, followed by a computer Monte Carlo (MC) simulation procedure in order to trace the fate of the ω-mesons and its decay products $\pi^0\gamma$ in the nuclear medium. Because our MC calculations represent complete event simulations it will be possible to take into account the actual experimental acceptance effects. In the following we shall carry out
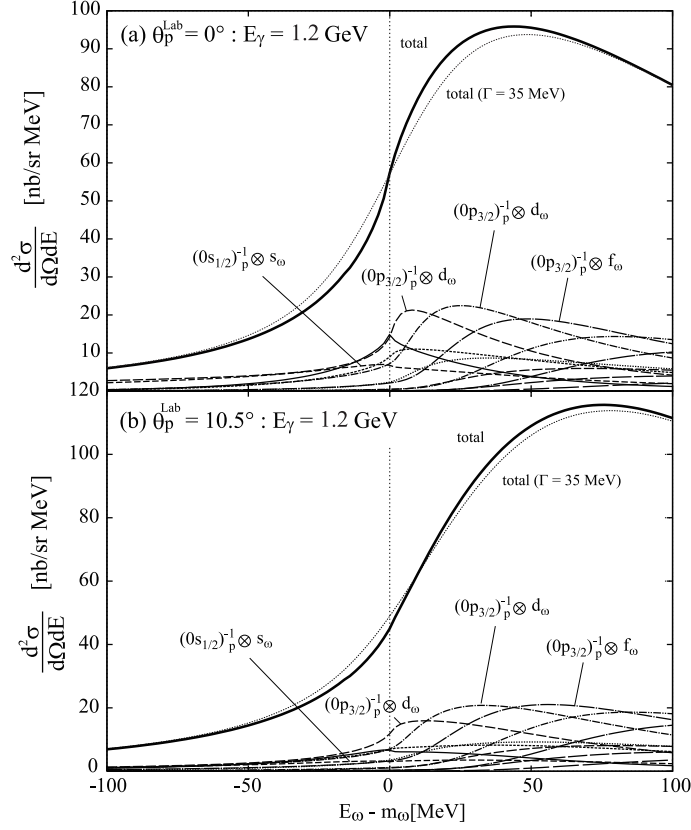
8

Figure 6: Same as Fig. 5 except for the potential depth $(V_0, W_0) = -(0, 50)$ MeV as in Eq. (2a).

the MC simulation taking into account the actual geometrical and kinematical acceptance conditions of the TAPS/Crystal Barrel experiment at ELSA.

In the MC calculations we shall impose the following cuts, both, for the elementary $p(\gamma, \omega \to \pi^0 \gamma)p$ and photonuclear $A(\gamma, \omega \to \pi^0 \gamma)X$ reactions:

C1) The ω-mesons are produced within an incident beam energy constrained by

$$1.5 \text{ GeV} \ < \ E_\gamma^{in} \ < \ 2.6 \text{ GeV}.$$

As in the actual experiment the incident photons are distributed according to the unnormalized bremsstrahlung spectrum

$$W(E_\gamma^{in}) \sim \frac{1}{E_\gamma^{in}}. \tag{3}$$

C2) The polar angle θ_p of the protons produced via a quasi-free kinematics is required to be detected in the range of
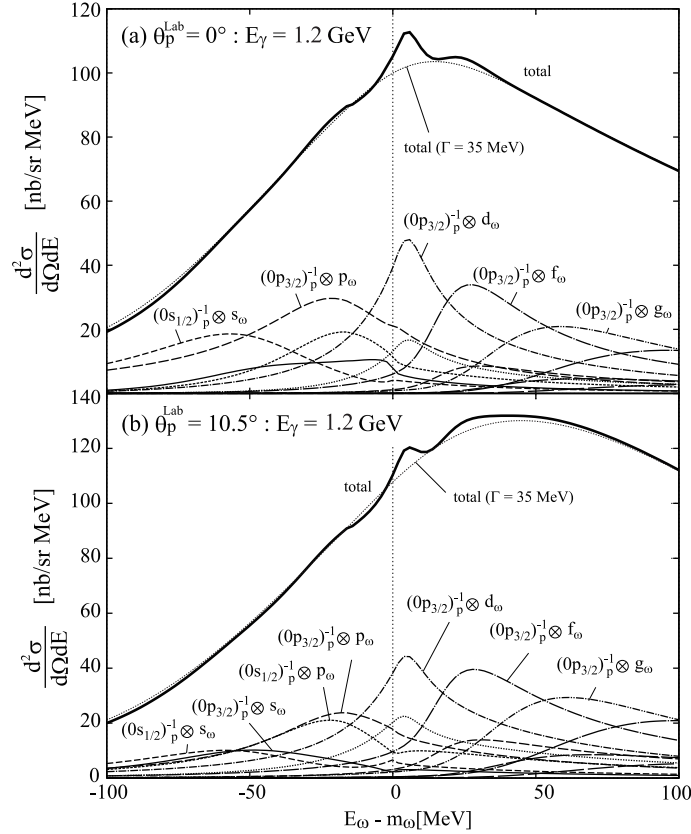
$$7° \ < \ \theta_p \ < \ 14°.$$

9

Figure 7: Same as Fig. 5 except for the potential depth $(V_0, W_0) = -(100, 50)$ MeV as in Eq. (2b).

C3) To increase the number of the $\omega \to \pi^0 \gamma$ decays inside the nucleus the three momentum of the $\pi^0 \gamma$ final state is restricted to values of

$$|\vec{p}_{\pi^0\gamma}| \; = |\vec{p}_{\pi^0} + \vec{p}_{\gamma}| \; < \; 400 \text{ MeV}.$$

Indeed, the fraction of the ω mesons decaying inside the nucleus can be optimized by minimizing the decay length $L_\omega = (p_\omega/m_\omega \Gamma_\omega)$ where Γ_ω is the width of the ω in the rest frame. It is therefore preferred that the kinetic energy of the ω-mesons reconstructed from $\pi^0 \gamma$ events with three momenta $\vec{p}_\omega = \vec{p}_{\pi^0} + \vec{p}_\gamma$ is small.

C4) The kinetic energy $T_{\pi^0} = E_{\pi^0} - m_{\pi^0}$ of the detected π^0 is taken to be larger than 150 MeV. This cut will strongly suppress the distorted events due to the quasielastic π^0 final state interactions (FSI) with the nucleons of the target.

C5) The energy of the photon in the $\pi^0 \gamma$ final state is larger than 200 MeV. This cut should attenuate the background channels.

We start our MC analysis with the cross section of the elementary reaction $\gamma p \to \omega p \to \pi^0 \gamma p$. In Ref. [41] the total cross section and the invariant differential cross sections $d\sigma_{\gamma p \to \omega p}/dt$ of the reaction (γ, ω) on protons were measured for incident photon energies from the reaction threshold $E_\gamma^{th} = m_\omega + m_\omega^2/2M_p \simeq 1.1$ GeV up to 2.6 GeV. We use this

experimental information in our analysis which is conveniently parametrized in Ref. [31]. In the following, the cross section on the neutron will be assumed to be the same as on a proton.

Our results for the differential cross section $d\sigma/dE_{\pi^0\gamma}$ as a function of the $E_{\pi^0\gamma} - m_\omega$ where $E_{\pi^0\gamma} = E_{\pi^0} + E_\gamma$, and after applying the experimental cuts listed above, are shown in Fig. 8. There are preliminary data for this reaction from the CBELSA/TAPS experiment. The lack of definitive data to which we could compare our results should not be an obstacle to discuss the theoretical results and draw some conclusions. Apart from the cross section from $\gamma p \to \omega p \to \pi^0 \gamma p$ that we evaluate, there should be background events from $\pi^0 \gamma p$ events where the $\pi^0 \gamma$ does not come from the decay of the ω. These and other background events are certainly present in the reaction, as shown in [30], and they have larger strength at invariant masses lower than m_ω. Correspondingly, there should be some background in the $\pi^0 \gamma$ energy distribution at lower energies than m_ω. We have evaluated the phase space for the $\gamma p \to p\pi^0\gamma$ reaction and find indeed strength at $\pi^0 \gamma$ energies below m_ω. There can also be other sources of background like from $\gamma p \to \pi^0\pi^0 p$, or $\gamma p \to \pi^0\eta p$, where one of the two photons from the decay of the π^0 or the η is not measured. We do not want to make a theory of the background here, but simply justify that a background like the one assumed in Fig. 8, peaking around $m_\omega - 100$ MeV is rather plausible. Indeed, this seems to be the case from the preliminary data of CBELSA/TAPS, with a background very similar to that drawn in Fig. 8. Yet, the conclusions of this section are not tied to specific details of this background but to general features which we discuss below. In Fig. 8 the solid histogram is obtained as a sum of the reconstructed exclusive events from the $\gamma p \to \omega p \to \pi^0 \gamma p$ reaction (dashed curve) and the background contribution. For the exclusive $\pi^0 \gamma$ events coming from $\gamma p \to \omega p \to \pi^0 \gamma p$ an experimental resolution of 50 MeV was imposed, see Ref. [30]. Note that the last two cuts in the list, $E_\gamma > 200$ MeV and $T_{\pi^0} > 150$ MeV, are irrelevant for the $\omega \to \pi^0 \gamma$ events since basically all of the MC events coming from this source fall in the kinematic regions allowed by these cuts.

In the photonuclear reaction $A(\gamma, \omega)X$ the ω-mesons are produced inside the nucleus according to their in-medium spectral function which includes the collisional broadening of the ω due to the quasielastic and absorption channels. For the quasielastic scattering of the ω we use the parametrisation of the $\omega N \to \omega N$ cross section given in Refs. [14, 22]. The in-medium quasielastic scattering does not lead to a loss of flux and therefore does not change the total nuclear cross section. But the later affects the ω momentum and energy distributions, keeping the ω meson inside the nucleus for a longer time. The loss of ω flux is related to the absorptive part of the ω-nucleus optical potential. In the following the absorption width of the ω will be taken in the form

$$\Gamma_{abs} \simeq 100 \,\text{MeV} \times \frac{\rho(r)}{\rho_0} \tag{4}$$

with no shift of the ω mass, as suggested by the analysis of [31], although this latter assumption is not relevant for the conclusions to be drawn. As will be shown in Ref. [42] (preliminary results are available in [33]), the in-medium ω width of $\simeq 100$ MeV at normal nuclear matter density explains the nuclear transparency ratio measured in Ref. [33].

(LH$_2$) E$^{in}_\gamma$ = 1.5 -2.6 GeV, 7° < θ$_p$ < 14°, p$_{\pi^0\gamma}$ < 400 MeV, p$_\gamma$ > 200 MeV, T$_{\pi^0}$ > 150 MeV
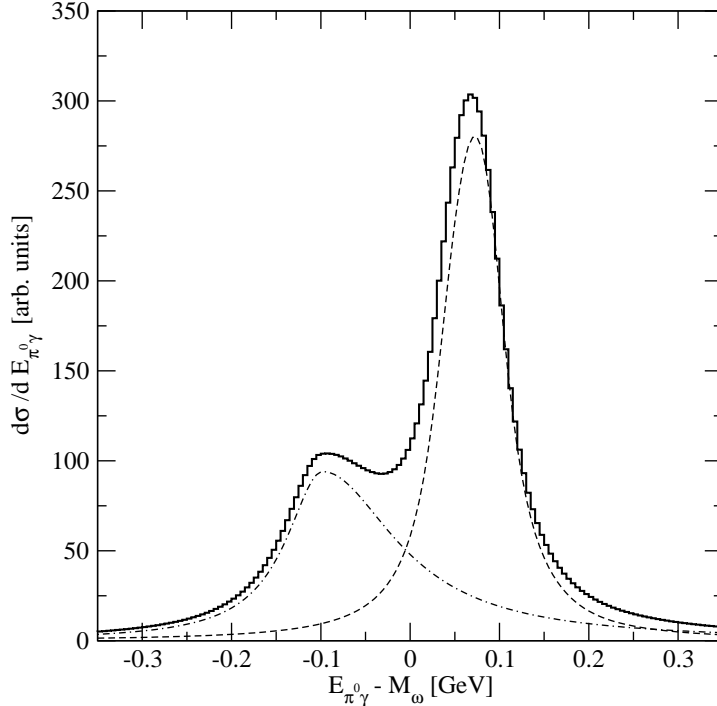
Figure 8: The differential cross section $d\sigma/dE_{\pi^0\gamma}$ of the reaction $\gamma p \to \pi^0 \gamma p$ as a function of the $E_{\pi^0\gamma} - m_\omega$ where $E_{\pi^0\gamma} = E_{\pi^0} + E_\gamma$. The spectrum (solid histogram) is obtained using the reconstructed $\pi^0\gamma$ events from the exclusive $\gamma p \to \omega(\pi^0\gamma)p$ reaction (dashed curve) plus an inclusive $\pi^0\gamma$ background discussed in the text (dash-dotted curve). The following cuts were imposed: $E_\gamma^{in} = 1.5 \div 2.6$ GeV, $7° < \theta_p < 14°$, $|\vec{p}_{\pi^0} + \vec{p}_\gamma| < 400$ MeV, $|\vec{p}_\gamma| > 200$ MeV and $T_{\pi^0} > 150$ MeV. The exclusive $\omega \to \pi^0\gamma$ signal has been folded with the 50 MeV experimental resolution.

Using the MC method of Ref. [31], which proceeds in a close analogy to the actual experiment, we trace the fate of the ω-mesons and their decay products in their way out of the nucleus. All standard nuclear effects like the Fermi motion of the initial nucleons and Pauli blocking of the final ones are taken into account. The ω-mesons are allowed to propagate inside the nucleus and at each step δL the reaction probabilities for different channels like the decay of the ω into $\pi^0\gamma$ and $\pi\pi\pi$ final states, quasielastic scattering and in-medium absorption are properly calculated. Since we are interested in $\pi^0\gamma$ events the absorption channels and decay $\omega \to \pi\pi\pi$ remove the ω-mesons from initial flux. The reconstructed $\pi^0\gamma$ events may come from both the ω decaying inside and outside the nucleus. If the resonance leaves the nucleus, its spectral function must coincide with the free distribution, because the collisional part of the width is zero in this case. When the ω decays into $\pi^0\gamma$ pair inside the nucleus its mass distribution is generated according to the in-medium spectral function at the local density. For a given mass $\widetilde{m}_\omega$ the ω-
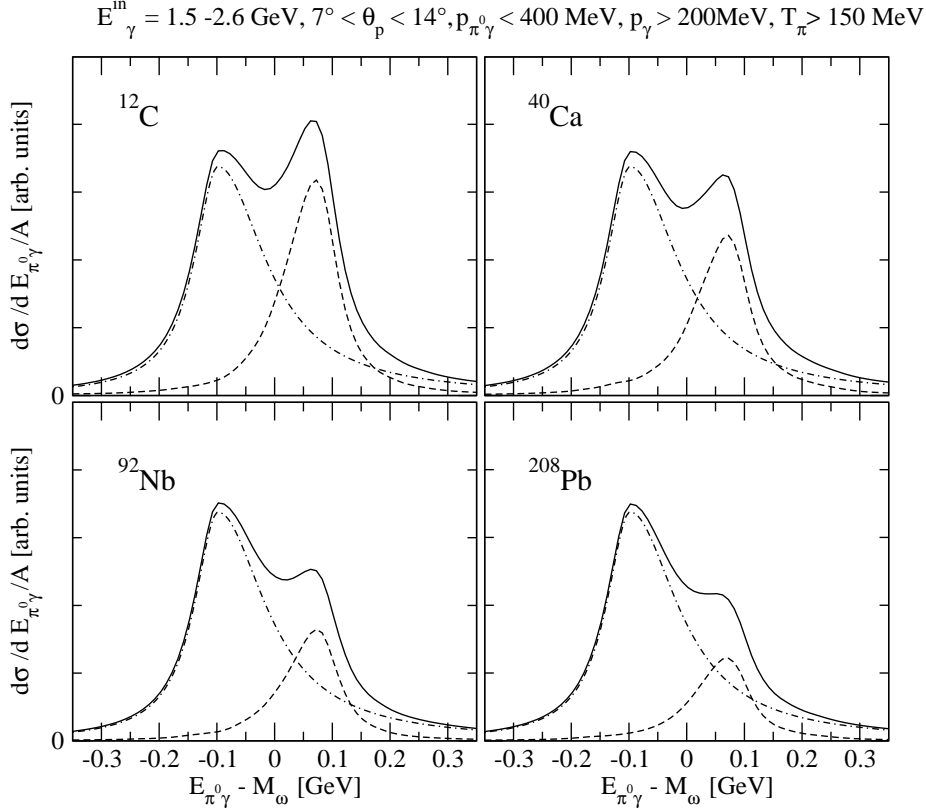
Figure 9: The differential cross section $d\sigma/dE_{\pi^0\gamma}$ of the reaction $A(\gamma, \pi^0\gamma)X$ as a function of $E_{\pi^0\gamma} - m_\omega$ from ^{12}C, ^{40}Ca, ^{92}Nb and ^{208}Pb nuclear targets. The reconstructed exclusive events from the $\omega \to \pi^0\gamma$ decay are shown by the dashed curves. The $\pi^0\gamma$ background is shown by the dash-dotted curves. The sum of the two contributions is given by the solid curves. The following cuts were imposed: $E_\gamma^{in} = 1.5 \div 2.6$ GeV, $7° < \theta_p < 14°$, $|\vec{p}_{\pi^0} + \vec{p}_\gamma| < 400$ MeV, $|\vec{p}_\gamma| > 200$ MeV and $T_\pi > 150$ MeV. The exclusive $\omega \to \pi^0\gamma$ signal has been folded with the 50 MeV experimental resolution. All spectra are normalized to the corresponding nuclear mass numbers A.

mesons are allowed to decay isotropically in the c.m. system into $\pi^0\gamma$ channel with a width $\Gamma_{\pi^0\gamma} = 0.76$ MeV. The direction of the π^0 (therefore γ) is then chosen randomly and an appropriate Lorentz transformation is done in order to generate the corresponding $\pi^0\gamma$ distributions in the laboratory frame. The ω-mesons are reconstructed using the energy and momentum of the $\pi^0\gamma$ pair in the laboratory.

The reconstruction of the genuine $\omega \to \pi^0\gamma$ mode is affected by the final state interactions of the π^0 in the nucleus. In this case, if the π^0 events come from the interior of the nucleus we trace the fate of the neutral pions starting from the decay point of the ω-meson. In their way out of the nucleus pions can experience the quasielastic scattering or can be absorbed. The intrinsic probabilities for these reactions as a function of the nuclear matter density are calculated using the phenomenological models of Refs [44, 45, 46], which also include higher order quasielastic cuts and the two-body and three-body absorption mechanisms. Note that

E^{in}_{γ} = 1.5 -2.6 GeV, $7° < \theta_p < 14°$, $p_{\pi^0\gamma} < 400$ MeV, $p_\gamma > 200$ MeV, $T_{\pi^0} > 150$ MeV
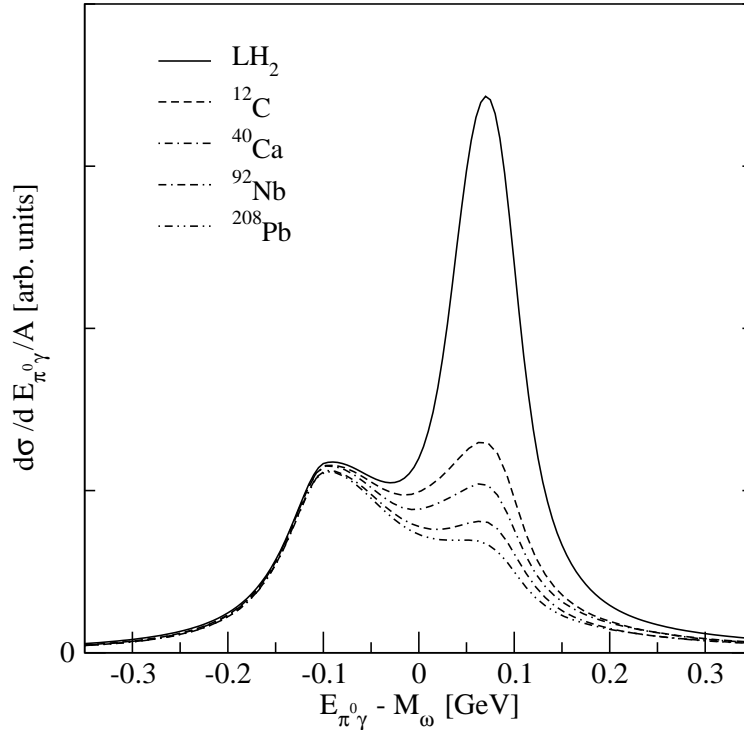

Figure 10: Summary plot of the reconstructed $\pi^0\gamma$ events in the reaction $(\gamma, \pi^0\gamma)$ from the proton target (solid) and sample nuclear targets ^{12}C (dashed), ^{40}Ca(dash-dotted), ^{92}Nb(dash-dash-dotted) and ^{208}Pb(dot-dot-dashed).

the FSI of the pions distorts the $\pi^0\gamma$ spectra and makes also an additional contribution to the negative part of the $E_{\pi^0\gamma} - m_\omega$ distribution. It was already demonstrated in Refs. [43, 20] that the contributions of the distorted events due to the FSI of the pions can be largely suppressed by using the cut on kinetic energy of pions $T_\pi > 150$ MeV. We confirm this finding and use it further in our analysis. Since the FSI of the γ quanta are rather weak they are allowed to escape the nucleus without distortion.

4   Results of the MC calculations

In the following we assume that the inclusive $\pi^0\gamma$ background scales with respect to the target nucleus mass number A like

$$\sigma_A \simeq A\, \sigma_{elem}. \tag{5}$$

This assumption implies merely a rather weak absorption of the inclusive $\pi^0\gamma$ pairs in the nuclear medium. Note that this assumption is supported by the present MC calculations

which show only the marginal effects due to the FSI of the relatively fast pions (beyond the $\Delta(1232)$ region). Recall that, because of the cuts we have imposed, the kinetic energies of the pions are always larger than $T_\pi > 150$ MeV. But this is not the case for the exclusive $\pi^0\gamma$ events coming from the decay of the $\omega \to \pi^0\gamma$. Although, the pions coming from this source are also fast and easily abandon the nucleus without significant FSI, the rather strong absorption of the ω inside the nucleus might change the scaling relation Eq. (5) and

$$\sigma_A(\omega \to \pi^0\gamma) \simeq A^\alpha \, \sigma_{elem}(\omega \to \pi^0\gamma) \tag{6}$$

where the attenuation parameter $\alpha < 1$.

In Fig. 9 we show the result of the MC simulation for the $E_{\pi^0\gamma} - m_\omega$ spectra reconstructed from the π^0 and γ events. The calculations are performed for the sample nuclear targets ^{12}C, ^{40}Ca, ^{92}Nb and ^{208}Pb. The kinematic and acceptance cuts discussed before have been already imposed. The MC distributions are normalized to the nuclear mass number A. The solid curves correspond to the sum of the inclusive $\pi^0\gamma$ background (dash-dotted curve), which is not related to the production and decay of the ω-mesons, and the exclusive $\pi^0\gamma$ events coming from the direct decay of the $\omega \to \pi^0\gamma$. The contributions of the exclusive $\omega \to \pi^0\gamma$ events are shown by the dashed curves. We note a very strong attenuation of the $\omega \to \pi^0\gamma$ signal with respect to the background contribution with increasing nuclear mass number A. This is primary due to the stronger absorption of the ω-mesons with increasing nuclear matter density, see Eq. (4). Also the contribution of the ω-mesons decaying inside the nucleus (with and without π^0 rescattering) is increasing as a function of mass number A merely due to an increase in the effective radius of the nucleus. In Fig. 10 we compare the nuclear cross sections of all sample nuclei with the $E_{\pi^0\gamma} - m_\omega$ spectra from the hydrogen target. Here one can see a double hump structure of the $E_{\pi^0\gamma} - m_\omega$ spectra but with the considerable attenuation of the exclusive $\omega \to \pi^0\gamma$ signal from light to heavy nuclei.

The former excercise indicates that given the particular combination of $\pi^0\gamma$ from an uncorrelated background and from ω decay, and the different behaviour of these two sources in the $\pi^0\gamma$ production in nuclei, a two bump structure seems unavoidable in nuclei. Should we have not done this calculation and intepreted it in the way we have done, the observation of a peak at about 100 MeV below the ω mass could easily tempt anyone to claim it as an indication of a bound ω state in the nucleus. By performing the present study we are paving the way for future investigations on the topic with the performance of the necessary simulation of conventional mechanisms which accompany the reactions used in the search for more exotic phenomena.

We would like to insist on the issue of the background, because there can be many sources for it. In the CBELSA/TAPS experiment, where the π^0 is observed from the two γ decay, a background of $\pi^0\gamma$ could also come from the production of two π^0, or $\pi^0\eta$, with no detection of a fourth γ coming from one π^0 or η decay. Such background could be eliminated, but there are unavoidable backgrounds like that coming from the $\gamma p \to p\pi^0\gamma$ reaction. Having this in mind we can easily see that even if the background of the reaction after eliminating avoidable backgrounds is about one third of the one assumed in the

present discussion, or even smaller, the two bump structure of Fig. 9 would still show up.

Finally, we would like to make a final comment in the sense that the strength of the cross section bears some information in itself. In the calculations done for the capture of ω mesons in bound orbits the cross sections are presented in absolute numbers. Should experiments find some peak structure in the ω bound region with a strength considerably larger than the one predicted in the present calculations, this would be an indication that the strength observed is coming from some sort of background, not from the formation of bound ω states.

5   Conclusions

In the present work we have carried out some calculations which should be very helpful in the search for eventual bound ω states in nuclei. In the first part we evaluated the reaction cross sections for the (γ, p) reaction in nuclei leading to the production of bound or unbound ω states together with the excitation of nuclear bound states. The calculations were done using different optical potentials which covered a wide range of bindings and absorptive parts. We found that only for potentials where the real part was larger than twice the imaginary part there was some chance to see peaks in the ω energy spectrum corresponding to the formation of the ω bound states. Clear peaks could be seen for a potential (-156, -29) MeV (at $\rho = \rho_0$), while if we had an imaginary part of about -50 MeV, as suggested by present experimental data on the A dependence of the ω production, even with 100 MeV binding no signal could be seen in the calculated spectrum. We studied the reaction for different photon energies and different proton angles. Since the optimal situation to see the peaks appears for recoilesss kinematics, the photon energy of 2 GeV was the optimal one if one observes protons in the forward direction. However, if the experimental conditions make it impossible or difficult to measure forward protons and a proton angle around 10 degrees is the choice, then we showed that a photon energy of about 1.2 GeV was more suited and led to better recoilles kinematics than with photons of 2 GeV. We performed the calculations for this situation which should serve to compare with experimental measurements made in the future.

Another relevant finding of the present work was that, even if bound states exist and they lead to peaks in the (γ, p) reaction, an experimental resolution better than 20 MeV in the ω energy is mandatory to make the peaks visible.

Finally we made another useful evaluation by calculating the inclusive (γ, p) reaction leading to $\pi^0 \gamma$ events. To the elementary reaction $\gamma p \to \omega p$ with subsequent $\pi^0 \gamma$ decay of the ω we added a certain background from reactions leading to $\pi^0 \gamma$ with not connection to ω production. Then we studied this reaction in nuclei, and because of the different behavior in the production of uncorrelated and ω correlated $\pi^0 \gamma$ pairs, we showed that a peak appeared in nuclei in the region of $\pi^0 \gamma$ energy around $m_\omega - 100$ MeV, which could easily be misidentified by a signal of a bound ω state in nuclei.

Altogether, the information found here should be of much help in order to identify the ideal set ups for future experiments searching for ω bound states in nuclei and to properly

interprete results of these experiments.

Acknowledgments

References

[1] M. Post, S. Leupold and U. Mosel, Nucl. Phys. A **741** (2004) 81 [arXiv:nucl-th/0309085].

[2] G. E. Brown and M. Rho, Phys. Rev. Lett. **66** (1991) 2720.

[3] T. Hatsuda and S. H. Lee, Phys. Rev. C **46** (1992) 34.

[4] V. Bernard and U. G. Meissner, Nucl. Phys. A **489** (1988) 647.

[5] H. Kurasawa and T. Suzuki, Prog. Theor. Phys. **84** (1990) 1030.

[6] H. C. Jean, J. Piekarewicz and A. G. Williams, Phys. Rev. C **49** (1994) 1981 [arXiv:nucl-th/9311005].

[7] F. Klingl, N. Kaiser and W. Weise, Nucl. Phys. A **624** (1997) 527 [arXiv:hep-ph/9704398].

[8] K. Saito, K. Tsushima, A. W. Thomas and A. G. Williams, Phys. Lett. B **433** (1998) 243 [arXiv:nucl-th/9804015].

[9] K. Tsushima, D. H. Lu, A. W. Thomas and K. Saito, Phys. Lett. B **443** (1998) 26 [arXiv:nucl-th/9806043].

[10] B. Friman, Acta Phys. Polon. B **29** (1998) 3195 [arXiv:nucl-th/9808071].

[11] F. Klingl, T. Waas and W. Weise, Nucl. Phys. A **650** (1999) 299 [arXiv:hep-ph/9810312].

[12] M. Post and U. Mosel, Nucl. Phys. A **688** (2001) 808 [arXiv:nucl-th/0008040].

[13] K. Saito, K. Tsushima, D. H. Lu and A. W. Thomas, Phys. Rev. C **59** (1999) 1203 [arXiv:nucl-th/9807028].

[14] G. I. Lykasov, W. Cassing, A. Sibirtsev and M. V. Rzyanin, Eur. Phys. J. A **6** (1999) 71 [arXiv:nucl-th/9811019].

[15] A. Sibirtsev, C. Elster and J. Speth, [arXiv:nucl-th/0203044].

[16] A. K. Dutt-Mazumder, R. Hofmann and M. Pospelov, Phys. Rev. C **63** (2001) 015204 [arXiv:hep-ph/0005100].

[17] M. F. M. Lutz, G. Wolf and B. Friman, Nucl. Phys. A **706** (2002) 431 [Erratum-ibid. A **765** (2006) 431] [arXiv:nucl-th/0112052].

[18] S. Zschocke, O. P. Pavlenko and B. Kampfer,0603013 Phys. Lett. B **562** (2003) 57 [arXiv:hep-ph/0212201].

[19] A. K. Dutt-Mazumder, Nucl. Phys. A **713** (2003) 119 [arXiv:nucl-th/0207070].0603013

[20] P. Muhlich, T. Falter and U. Mosel, Eur. Phys. J. A **20** (2004) 499 [arXiv:nucl-th/0310067].

[21] P. Muehlich, V. Shklyar, S. Leupold, U. Mosel and M. Post, [arXiv:nucl-th/0607061].

[22] P. Muhlich and U. Mosel, Nucl. Phys. A **773** (2006) 156 [arXiv:nucl-th/0602054].

[23] B. Steinmueller and S. Leupold, arXiv:hep-ph/0604054.

[24] R. Arnaldi *et al.* [NA60 Collaboration], Phys. Rev. Lett. **96** (2006) 162302 [arXiv:nucl-ex/0605007].

[25] U. Mosel, Prog. Part. Nucl. Phys. **42** (1999) 163 [arXiv:nucl-th/9812067].

[26] K. Ozawa *et al.* [E325 Collaboration], Phys. Rev. Lett. **86** (2001) 5019 [arXiv:nucl-ex/0011013].

[27] T. Tabaru *et al.*, Phys. Rev. C **74** (2006) 025201 [arXiv:nucl-ex/0603013].

[28] F. Sakuma *et al.* [E325 Collaboration], arXiv:nucl-ex/0606029.

[29] D. Weygand, talk at the QNP06 Conference, Madrid, June 2006.

[30] D. Trnka *et al.* [CBELSA/TAPS Collaboration], Phys. Rev. Lett. **94** (2005) 192303 [arXiv:nucl-ex/0504010].

[31] M. Kaskulov, E. Hernandez and E. Oset, [arXiv:nucl-th/0610067].

[32] E. Marco and W. Weise, Phys. Lett. B **502** (2001) 59 [arXiv:nucl-th/0012052].

[33] D. Trnka, PhD Thesis, University of Giessen, 2006.

[34] R.S. Hayano, S. Hirenzaki, A. Gillitzer, Eur. Phys. J. A 6 (1999) 99.

[35] O. Morimatsu, K. Yazaki, Nucl. Phys. A 435 (1985) 727; O. Morimatsu, K. Yazaki, Nucl. Phys. A 483 (1988) 493.

[36] D. Jido, H. Nagahiro, S. Hirenzaki, Phys. Rev. C 66 (2002) 045202; H. Nagahiro, D. Jido, S. Hirenzaki, Phys. Rev. C 68 (2003) 035205; H. Nagahiro, D. Jido, S. Hirenzaki, Nucl. Phys. A 761 (2005) 92.

[37] H. Nagahiro, M. Takizawa, S. Hirenzaki, Phys. Rev. C in print, [arXiv:nucl-th/0606052].

[38] H. Toki, S. Hirenzaki, T. Yamazaki, Nucl. Phys. A 530 (1991) 679; S. Hirenzaki, H. Toki, T. Yamazaki, Phys. Rev. C 44 (1991) 2472.

[39] S. Hirenzaki, E. Oset, Phys. Lett. B 527 (2002) 69.

[40] H. Gilg, *et al.*, Phys. Rev. C 62 (2000) 025201; K. Itahashi, *et al.,* Phys. Rev. C 62 (2000) 025202; H. Geissel, *et al.*, Phys. Rev. Lett. 88 (2002) 122401; K. Suzuki, *et al.*, Phys. Rev. Lett. 92 (2004) 072302.

[41] J. Barth, *et al.*, Eur. Phys. J. A 18 (2003) 117.

[42] D. Trnka et al., to be published.

[43] J. G. Messchendorp, A. Sibirtsev, W. Cassing, V. Metag and S. Schadmand, Eur. Phys. J. A **11**, 95 (2001) [arXiv:hep-ex/0106041].

[44] L. L. Salcedo, E. Oset, M. J. Vicente-Vacas and C. Garcia-Recio, Nucl. Phys. A **484** (1988) 557.

[45] E. Oset, L. L. Salcedo and D. Strottman, Phys. Lett. B **165**, 13 (1985).

[46] E. Oset and D. Strottman, Phys. Rev. C **42**, 2454 (1990).